Trans Stimulation Provides Evidence for a Drug Efflux Carrier as the Mechanism of Chloroquine Resistance in *Plasmodium falciparum*†

Cecilia P. Sanchez,‡ Wilfred Stein,§ and Michael Lanzer*,‡

Hygiene Institut, Abteilung Parasitologie, Universität Heidelberg, Im Neuenheimer Feld 324, D-69120 Heidelberg, Germany, and Biological Chemistry, Silberman Institute of Life Sciences, Hebrew University of Jerusalem, Givat Ram, Jerusalem 91904, Israel

Received February 17, 2003; Revised Manuscript Received May 13, 2003

ABSTRACT: The mechanism underpinning chloroquine drug resistance in the human malarial parasite *Plasmodium falciparum* has remained controversial. Currently considered models to explain the resistance phenotype include acquisition of a chloroquine efflux pump, changes in intracellular chloroquine partitioning, diminished binding affinity of chloroquine to its intracellular target, heme, and changes in heme crystallization. To challenge these different models, we have investigated chloroquine accumulation under trans-stimulation conditions and in the presence and absence of glucose. We show that, in chloroquine-sensitive strains, labeled chloroquine accumulation is steadily reduced as the pre-equilibrated chloroquine concentration is raised. In the resistant cells, the extent of accumulation is, strikingly, raised at the lower levels of preloading, in comparison with resistant controls in the absence of chloroquine. The trans-stimulation effect observed in chloroquine-resistant cells is strictly energy-dependent. The data are interpreted in terms of a model in which chloroquine is bound to intracellular binding sites, not different as between sensitive and resistant cells, but where, in resistant cells, there exists an energy-dependent carrier that moves chloroquine out of this intracellular compartment. A mathematical model describing the kinetics of these processes is presented.

Chloroquine, once the first-line antimalaria drug in the global campaign against malaria, now frequently fails in the field because of widespread resistance. As affordable alternatives to chloroquine (CQ)[1] are not available, the incidence of malaria has steadily increased during the last two decades to today's staggering figures of an estimated 300−500 million clinical cases and 1−3 million deaths annually (*1*). In an effort to develop drugs that reverse or circumvent chloroquine resistance, the molecular mechanism(s) underpinning this phenotype has been intensely investigated in the human malarial parasite *Plasmodium falciparum* during the past decades, yet the nature of this resistance has remained controversial.

Chloroquine's mode of action is intricately linked with the parasite's heme metabolism (*2*). During development within human erythrocytes, *P. falciparum* feeds on the host cell's hemoglobin, which is taken up by the parasite and digested within acidic vacuoles. The heme moiety released during hemoglobin degradation inhibits the activity of several enzymes (*3*, *4*) and destabilizes membranes by promoting lipid peroxidation (*5*) and facilitating ion exchange (*6*). The parasite neutralizes this toxin through three independent pathways: peroxidative decomposition (*7*), glutathione-dependent degradation (*8*, *9*), and crystallization to insoluble and inert hemozoin (*10*). Chloroquine, which accumulates to mM concentrations within the food vacuole, forms a stable complex with heme (*5*, *11*, *12*), resulting in a buildup of toxic membrane-associated heme−chloroquine complexes that eventually destroy the integrity of the parasite's membranes (*13*−*17*).

As the parasite must degrade hemoglobin both to meet its nutrient requirements and to counteract osmotic imbalances within the host erythrocyte resulting from its own anabolic activities (*18*), the production of heme cannot be avoided. Accordingly, cell-free extracts prepared from chloroquine-sensitive (CQS) and chloroquine-resistant (CQR) *P. falciparum* strains bind similar levels of chloroquine (*19*, *20*). In vivo, however, CQR parasite strains accumulate significantly less chloroquine than do CQS strains (*21*, *22*). These findings limit the possible drug resistance mechanisms to those that prevent the encounter of chloroquine with heme (*20*). On the basis of these considerations, three alternative models have been formulated to explain the chloroquine resistance phenotype.

The first model proposed the acquisition of an active verapamil-sensitive efflux pump, similar to P-glycoproteins of multidrug-resistant cancer cells, which would expel incoming chloroquine from the cell (*23*−*27*). While the initial report showed an accelerated chloroquine efflux in CQR

† This work was supported by a grant from the Deutsche Forschungsgemeinschaft (LA 941/4).

* To whom correspondence should be addressed. Abteilung Parasitologie, Universitätsklinikum Heidelberg, Im Neuenheimer Feld 324, 69120 Heidelberg, Germany. Phone: +49 6221 567845. Fax: +49 6221 564643. E-mail: michael_lanzer@med.uni-heidelberg.de.

‡ Universität Heidelberg.

§ Hebrew University of Jerusalem.

[1] Abbreviations: CQ, chloroquine; CQS, chloroquine-sensitive; CQR, chloroquine-resistant; K_b, dissociation constant between chloroquine and its intracellular binding site (Michaelis constant); K_p, apparent binding constant of chloroquine to the efflux carrier (Michaelis constant); r_o, pump-to-leak ratio.

10.1021/bi034269h CCC: $25.00
Published on Web 07/11/2003

parasite strains, as compared to that in CQS parasite strains (*25*), subsequent studies failed to corroborate this finding (*28*, *29*). Moreover, epidemiological surveys revealed only a vague association between chloroquine resistance and mutations and/or amplification of the *P. falciparum* multidrug resistance gene 1 (*mdr1*) (*30*−*36*), while a genetic cross done between a CQS and a CQR clone found no linkage at all (*37*). Instead, the cross revealed that chloroquine resistance is causatively linked with polymorphisms within a gene of hitherto unknown function, termed *pfcrt* (*38*).

The second model invoked differences in chloroquine partitioning as the basis of the drug-resistant phenotype. Chloroquine, which is a lipophilic, diprotic weak base, readily crosses membranes by passive diffusion to accumulate in the acidic compartments, such as the parasite's food vacuole, where it binds to heme (*39*, *40*). As chloroquine uptake would depend on the pH gradient between the external medium (pH = 7.3) and the vacuole (pH ≈ 5.4), elevation in the vacuolar pH would reduce acidotropic accumulation of chloroquine (*40*, *41*). However, differences in vacuolar pH between CQS and CQR parasite strains have not been found (*42*−*44*), with the exception of one study, which surprisingly reported a more acidic pH for the food vacuole of CQR parasites as compared to that of CQS parasites, contrary to the partitioning model (*45*). These latter authors interpreted their finding by suggesting that heme aggregates and crystallizes better at an acidic pH, which in turn would reduce the amount of heme available as a target for chloroquine (*46*, *47*). Several subsequent studies have questioned the conclusions drawn by this study (*42*, *48*), in particular casting doubt on the validity of the fluorimetric approach used to determine vacuolar pH values by pointing out that the parasite's food vacuole is extremely sensitive to photolysis (*49*).

The third model suggests that CQR strains reduce the affinity of chloroquine to heme through the intervention of a heme-binding protein such that this protein reduces access of chloroquine to its target (*20*, *50*−*52*). Despite its overall appeal, this model suffers from a lack of genetic and biochemical data, demonstrating that heme-binding proteins of parasite origin, such as the histidine-rich protein 2 (*11*, *53*), have altered binding specificities for heme in CQR *P. falciparum* strains as compared to those in CQS strains.

The debate on the mode of chloroquine resistance is fueled by a lack of solid biochemical and kinetic data on chloroquine uptake and accumulation, resulting from difficulties in obtaining pure populations of *P. falciparum*-infected erythrocytes. Until now kinetic studies have solely relied on cell culture material containing only 5−10% parasitized erythrocytes and 90% or more of uninfected erythrocytes. The contribution of the large amount of uninfected erythrocytes to the outcome of kinetic studies has been largely ignored. Here we have employed a recently described magnetic purification protocol to obtain pure populations of *P. falciparum*-infected erythrocytes (*54*). This enabled us to design a set of simple kinetic experiments to challenge the various models proposed for chloroquine drug resistance. Our data are inconsistent with the partitioning model and the diminished-binding model, but favor the presence of an energy-dependent chloroquine efflux pump as the basis of chloroquine resistance in *P. falciparum*.

EXPERIMENTAL PROCEDURES

Materials. [^{3}H]-Chloroquine diphosphate (18.8 Ci/mmol), [^{3}H]-hypoxanthine (17.9 Ci/mmol), and NCS-II tissue solubilizer were supplied by Amersham International. Chloroquine, verapamil, and glucose- and bicarbonate-free RPMI 1640 supplemented with 25 mM HEPES-Na and 2 mM glutamine were purchased from Sigma. Bicarbonate-free RPMI 1640 containing 11 mM glucose and supplemented with 25 mM HEPES-Na and 2 mM glutamine was purchased from Gibco. The ATP assay kit was purchased from Calbiochem.

P. falciparum Cultures. The *P. falciparum* clones HB3, Dd2, S106, and FCB were cultured as described (*55*) and synchronized using the sorbitol method (*56*). The genotypes of the strains used were confirmed by microsatellite analysis with the markers C2 M22, B5 M122, B7 M78, and PfRRM, as described (*57*). The susceptibility of the strains to chloroquine was determined as described (*58*). *P. falciparum*-infected erythrocytes were purified using a strong magnet (VarioMACS, Miltenyi Biotec, Germany), as described (*54*). This yielded a purity of trophozoite-infected erythrocytes of 98−100% as determined by microscopic examination of Giemsa-stained blood smears.

Trans-Stimulation Assay. Magnet-purified trophozoite-infected erythrocytes were resuspended in reaction buffer A (bicarbonate-free RPMI 1640 containing 11 mM glucose and supplemented with 25 mM HEPES-Na and 2 mM glutamine, pH 7.3 at 37 °C) at a hematocrit of 30 000 cells/μL. The hematocrit was determined by using a Neubauer counting chamber. The cells were then incubated at 37 °C for 15 min in the presence of different preloading chloroquine concentrations ranging from 0 to 10.0 μM. After preloading, cells were washed twice in ice-cold reaction buffer A (pH adjusted to 7.3 at 4 °C) and then resuspended in prewarmed reaction buffer A containing 43 nM [^{3}H]-chloroquine. The reaction was held at 37 °C, and the time course of [^{3}H]-chloroquine accumulation was monitored. Duplicative 75 mL aliquots were removed from the reaction at various time points and diluted with an equal volume of ice-cold reaction buffer A. These aliquots were immediately spun through a layer of a 5:4 mixture of dibutyl phthalate and dioctyl phthalate (15000*g*, 5 s) to separate the cells from the aqueous medium, which contained the unincorporated [^{3}H]-chloroquine. The aqueous phase was removed from each sample, and its radioactivity was determined to obtain an accurate measurement of the extracellular [^{3}H]-chloroquine concentration in each reaction. The cell pellets were recovered by cutting the reaction tubes through the oil layer. The tips of the tubes containing the cell pellets were placed in a larger 1.5 mL Eppendorf tube and incubated with 66 mL of ethanol and 33 mL of tissue solubilizer overnight at 55 °C. The lysates were decolorized by the addition of 25 mL of 30% H_2O_2 and acidified by the addition of 25 mL of 1 N HCl. The lysates were transferred to scintillation vials, and the radioactivity was measured using a liquid scintillation counter (TRI-CARB 2100 TR, Packard). The intracellular chloroquine concentration was calculated from the amount of [^{3}H]-chloroquine taken up by the cells and by assuming that the volume of a trophozoite-infected erythrocyte is 75 fL (*59*). Chloroquine accumulation was then expressed as the ratio of the intracellular versus the extracellular chloroquine

concentration (CQ_{in}/CQ_{out}). Where indicated, trans-stimulation experiments were performed under glucose-free conditions in reaction buffer B (glucose- and bicarbonate-free RPMI 1640 supplemented with 25 mM HEPES-Na and 2 mM glutamine). Cells were held in reaction buffer B for 10 min to deplete them of intracellular ATP prior to the commencement of the experiment.

Energy Dependence of [^{3}H]-Chloroquine Flux. Magnet-purified trophozoite-infected erythrocytes were resuspended in reaction buffer B at a hematocrit of 30 000 cells/μL and incubated at 37 °C in the presence of 43 nM of [^{3}H]-chloroquine. At the time points indicated, duplicative 75 μL aliquots were withdrawn and analyzed as described above. After 20 min of incubation, the reaction was split in half. To one half, glucose was added to a final concentration of 11 mM, and the time course of [^{3}H]-chloroquine flux was monitored in both halves of the experiment, as described above. The amount of [^{3}H]-chloroquine taken up was calculated and normalized to 1×10^6 infected erythrocytes.

Measurement of Intracellular ATP. The concentration of ATP within the parasite was measured using the ATP-Assay kit (Calbiochem) as described by the manufacturer.

[^{3}H]-Chloroquine Uptake Assay. The kinetic studies on chloroquine uptake at initial rates were done as previously described (*60*).

Curve Fitting. Kinetic data were analyzed using computerized least-squares fit methods (Sigma Plot 2001, Jandel Corporation).

Theory of Chloroquine Uptake Kinetics. Our model takes three aspects of chloroquine accumulation into consideration: (i) the increased distribution of chloroquine within the food vacuole, as compared with its concentration in the external medium, as a result of the pH gradient between the vacuole and the cell exterior, (ii) the binding of chloroquine to its intracellular binding sites, and (iii) the effect of an outwardly directed pump on intracellular/extracellular chloroquine distribution. We assume that for both sensitive and resistant cells, the pH gradient and the amount of intracellular binding site material are not different. Denoting the concentration of free intracellular chloroquine as S_i, the total binding capacity of the chloroquine-binding component inside the cell as Tot, the half-saturation constant for binding as K_b, and with the concentration of bound chloroquine as ES_i, at the prevailing pH gradient, we can write:

$$ES_i = \frac{S_i \mathrm{Tot}}{K_b + S_i} \tag{1}$$

The term K_b contains within it both the intrinsic affinity of the chloroquine-binding site for its substrate and also the effect of the pH gradient between the extracellular medium and the compartment where chloroquine is bound. Consider now the effect of an outwardly directed pump on the distribution of chloroquine. Chloroquine enters and leaves the cell by simple diffusion with a rate constant p, the same for both directions. In addition, it leaves the cell through the action of the pump, which acts on it with a rate constant k. Then, with S_o as the extracellular concentration of chloroquine, the distribution ratio of chloroquine is given by

$$\frac{S_i}{S_o} = \frac{p}{p + k} \tag{2}$$

Bray et al. (*20*) demonstrated that binding constants determined in experiments such as those of Figure 6 in the present paper on drug-sensitive parasites were very similar to binding constants directly derived from binding of chloroquine to heme in cell debris, measured in free solution. This suggests that the concentration of free chloroquine within the drug accumulation compartment in the sensitive parasite is indeed the same as that in the external medium. This is consistent with the parameter k being equal to zero in the drug-sensitive cells. Substituting for S_i from eq 2 into eq 1 and simplifying, we obtain:

$$ES_i = \frac{S_o \mathrm{Tot}}{K_b \dfrac{p + k}{p} + S_o} \tag{3}$$

We write $(p + k)/p$ as r, which is equal to (1 + the pump-to-leak ratio) and a useful parameter in what follows. Equation 3 becomes:

$$ES_i = \frac{S_o \mathrm{Tot}}{K_b r + S_o} \tag{4}$$

It will immediately be obvious that eq 4 enables us to define an apparent binding constant K_{app}, which expresses the dependence of the total chloroquine bound intracellularly, ES_i, at the prevailing pH gradient, as a function of the extracellular concentration of chloroquine, S_o. The parameter K_{app} is clearly equal to r times K_b. Thus, as the pump-to-leak ratio increases, so will the apparent binding constant for chloroquine increase, in strict linear fashion with p/k.

We must assume, however, that the chloroquine pump has its own dependence on the concentration of chloroquine and that it operates on chloroquine, as pumps do in general, with its rate having a hyperbolic (Michaelian) dependence on chloroquine concentration, with half-saturation concentration of K_p. We can write, with k_o as the maximum velocity of pumping,

$$k = \frac{S_i k_o}{S_i + K_p} \tag{5}$$

Substituting for k, the operative rate constant at any S_i, from this equation into eq 2 and simplifying, we obtain:

$$\frac{S_i}{S_o} = \frac{K_p + S_i}{K_p r_o + S_i} \tag{6}$$

where now r_o is equal to (1 + the pump leak ratio), in terms of the maximum value of the pump rate constant k_o. This is a quadratic equation for S_i in terms of S_o, K_p, and r_o. This can be solved and rewritten to give

$$\frac{S_i}{S_o} = \frac{(1 - Q) \pm \sqrt{(1 - Q)^2 + 4 r_o Q}}{2 r_o} \tag{7}$$

where Q is K_p/S_o. In preliminary analyses of the data, it was

found that far better graphic fits to the data could be obtained if it was assumed that the postulated pump acts in a cooperative fashion upon its substrate chloroquine. With a Hill number of n, we write Q in eq 7 as

$$Q = \frac{K_p}{(S_i)^n} \tag{8}$$

A stoichiometry of 2 (i.e., with $n = 2$) was found to give excellent fits to the data.

Equation 7 gives the steady-state ratio of chloroquine in terms of the pump-to-leak ratio and of the ratio of K_p to S_o. Dividing the top and bottom of the right-hand side of eq 1 by S_o, writing S_i/S_o as R and K_b/S_o as B, we obtain

$$ES_i = \frac{R\mathrm{Tot}}{B + R} \tag{9}$$

Since R is given exactly by eq 7 and can be substituted into eq 9, we now have the full solution of the amount of accumulation of chloroquine intracellularly, ES_i, at the prevailing pH gradient in terms of the parameters Tot, K_b, K_p, and r_o, and of the extracellular chloroquine concentration, S_o. Of the four parameters, Tot and K_b can be found from binding experiments done on the drug-sensitive parasites where, by assumption, there is negligible drug pumping. The remaining two parameters, K_p and r_o, can then be found from experiments using resistant parasites and were calculated using computerized least-squares fit methods (Sigma Plot, Jandel Corporation).

Equations 1 and 4 can readily be transformed into forms that describe the accumulation of label, at the steady state, as a function of preloaded chloroquine, as required by the experiments of Figures 2−5 of this paper. We assume that the concentration of the labeled drug is low in comparison with the saturation constants K_b and K_p. It is then sufficient to replace the terms in S in the numerator of these equations by K_b, the drug-binding constant. We obtain for the sensitive cells

$$\frac{S_i}{S_o} = \frac{\mathrm{Tot}K_b}{K_b + S_o} \tag{10}$$

with S_o now being the concentration of preloaded chloroquine, while for the resistant cells

$$\frac{S_i}{S_o} = \frac{\mathrm{Tot}K_b}{K_b + S_i} \tag{11}$$

S_i is again the concentration of free drug and is obtained using eq 7.

The above equations can be modified to take into account a binding component that does not saturate in the concentration range studied. All that needs to be done is to add a factor TS to the right-hand side of each equation, where TS is the contribution of the nonsaturable component at any concentration S. Note that the derivation of these equations does not assume any special mechanism for the chloroquine pump. Pumping may be by a primary ATP-consuming pump or by a secondary pumping system in which chloroquine transport is linked to the movement of some other transportable substrate, down its concentration gradient that is established by an energy-dependent process.

RESULTS

Chloroquine Accumulation Is Energy Dependent. We initially reexamined the observation that chloroquine handling is energy dependent in both CQS and CQR *P. falciparum* strains (*44*, *61*), using our transport assay. Two *P. falciparum* clones were investigated: Dd2, a CQR parasite from Indochina ($IC_{50} = 137.0 \pm 11.0$ nM), and HB3, a fully chloroquine-susceptible clone from Honduras ($IC_{50} = 16.0 \pm 1.0$ nM). Purified erythrocytes infected with trophozoites (purity exceeding 98%) were incubated with 43 nM of [^{3}H]-chloroquine, and the time course of uptake was monitored. At the 20 min time point, glucose was or was not added to a final concentration of 11 mM and incubation continued. Again, the amount of [^{3}H]-chloroquine taken up was monitored over time. Figure 1 depicts the means and standard errors of nine such experiments performed over several weeks. In three experiments, the ATP levels in the cells were measured, with the results shown in the lower half of the figure. The chloroquine uptake was very similar in the two strains investigated during the initial 20 min incubation in the absence of glucose. After glucose was added, however, the time courses of chloroquine uptake showed marked differences between HB3 and Dd2. Chloroquine accumulated to an increased extent in the CQS strain, but left the cells in the CQR strain.

Curve fitting of the uptake curves, before glucose addition, to a simple exponential uptake curve gave the results collected in Table 1, where it can be seen that the rate constant of uptake is much the same for the two strains investigated. After glucose addition, the increased accumulation in the CQS strain again follows a simple exponential uptake curve. The data obtained by curve fitting (Table 1) suggest that the rate of uptake is slower, but not much slower, during this time period than it was for the first 20 min in the absence of glucose in both the CQS and CQR strain. After glucose addition, however, the rate of loss of chloroquine from the resistant strain fits a simple exponential *efflux* curve with a rate constant of 0.17 ± 0.02 min^{-1} (Table 1). The rates of accumulation of ATP in both the sensitive and the resistant strain (Figure 1, c and d) again fit simple exponential uptake curves (Table 1). Interestingly, the rate of accumulation of ATP in the CQR strain Dd2 (0.11 ± 0.01 min^{-1}) is fairly close to the rate of loss of chloroquine from the resistant cells. A possible interpretation of this finding is presented in the discussion.

Trans Stimulation Reveals Fundamental Differences in Chloroquine Flux between CQS and CQR Strains. To investigate further the differences in chloroquine accumulation between CQS and CQR strains, we performed a series of experiments in which erythrocytes infected with trophozoites of HB3 or Dd2 were pre-equilibrated with unlabeled chloroquine at different concentrations, ranging from 0.1 to 10 μM, (or without chloroquine for the controls) for 15 min before the cells were washed and placed in media containing 43 nM of [^{3}H]-chloroquine. This is the so-called trans-acceleration or trans-stimulation procedure, much used in classical transport studies (*62*). We reasoned that the unlabeled chloroquine would compete with the labeled

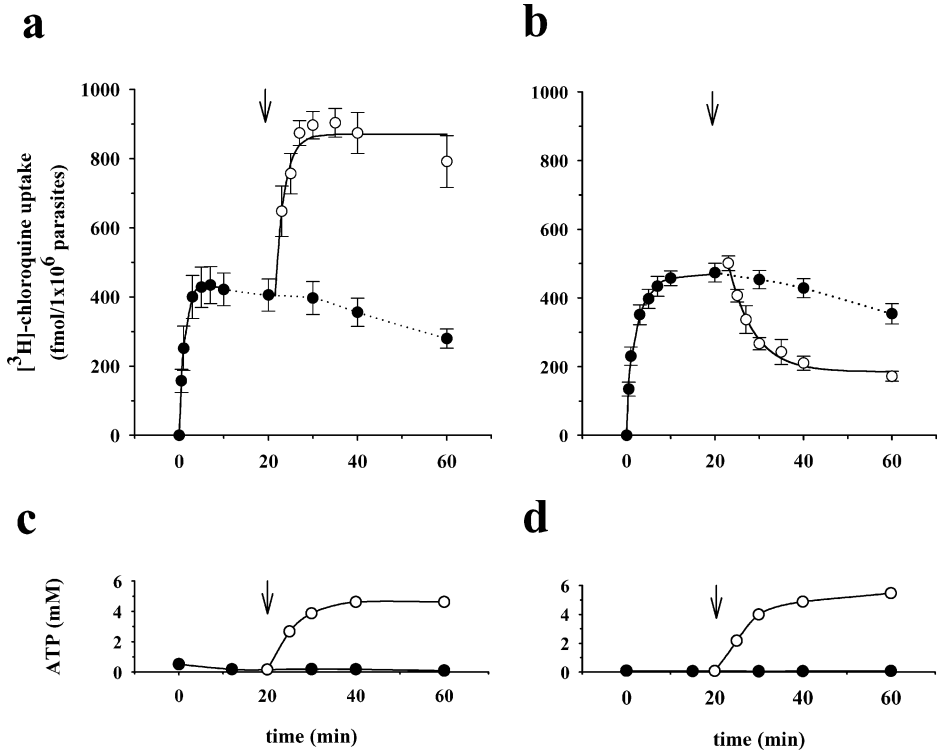

FIGURE 1: Energy dependence of chloroquine flux in *P. falciparum.* Temporal changes in radiolabeled chloroquine accumulation were monitored in the (a) CQS strain HB3 and the (b) CQR strain Dd2, in glucose-free medium (●) and after addition of glucose (○). An arrow indicates the time point of glucose addition. The means ± SE of nine independent determinations are shown. Data points used for curve fitting are connected by solid lines. The intracellular ATP concentration under these experimental conditions are given in (c) for HB3 and (d) for Dd2. A representative example of three independent determinations is shown. The kinetic parameters calculated from the fitted curves are compiled in Table 1.

Table 1: Kinetic Parameters for Chloroquine Uptake and Efflux and Intracellular ATP Accumulation in Different *P. falciparum* Strains[a]

		CQ uptake rate			
strain	status	−glucose min^{-1}	+glucose min^{-1}	CQ efflux rate min^{-1}	ATP production rate min^{-1}
HB3	CQS	0.89 ± 0.02 (9)	0.49 ± 0.12 (9)		0.17 ± 0.01 (3)
S106	CQS	0.32 ± 0.05 (4)	0.37 ± 0.06 (4)		n.d.[b]
Dd2	CQR	0.62 ± 0.08 (8)		0.17 ± 0.02 (8)	0.11 ± 0.01 (3)
FCB	CQR	0.44 ± 0.05 (5)		0.11 ± 0.02 (5)	n.d.[b]

[a] The values represent the means ± SE of *n* independent determinations and are derived from curve fitting of the data shown in Figures 1 and 5. [b] Not determined.

chloroquine at the intracellular binding sites in both the resistant and the sensitive cells, but that in the resistant cells it might, in addition, by trans stimulation compete with the system that lowers the intraparasite chloroquine concentration. The results of such experiments are depicted in Figure 2, with Figure 2a being the experiments with the CQS strain HB3 and Figure 2b showing the data for the CQR strain Dd2. For clarity, only the points for the controls (cells that did not receive unlabeled chloroquine) are connected by dotted lines. In all cases, the level of [^{3}H]-chloroquine increases with time to a maximum and then falls again, the descending portion arising, presumably, from the loss of both the labeled and the unlabeled chloroquine from the cells. In separate studies, we measured the rate of loss of the chloroquine that had been preloaded and found that at least one half was lost during 20 min of incubation (data not shown).

A clear difference is apparent, however, between the results for the CQS and the CQR strain. For the CQS strain HB3, the points for all the cells pre-equilibrated with chloroquine fall below the controls. Thus, the pre-equilibrated chloroquine appears to compete with the labeled chloroquine for binding to the intraparasite binding sites. For the CQR strain Dd2 this is not the case. The points for cells that were pre-equilibrated with chloroquine at the lower levels rise above the control levels. It would appear that, at these low levels of intracellular chloroquine, the chloroquine *enhances* the uptake of label. At the higher chloroquine levels, the system approaches that of the CQS cells in that unlabeled chloroquine apparently now competes with the intraparasite binding sites.

Changing the probing [^{3}H]-chloroquine concentration from 43 to 4 nM (below the IC_{50} value of HB3) or 400 nM (above the IC_{50} value of Dd2) had no significant effect on the outcome of the preloading experiment (data not shown). In other control experiments we monitored rhodamine 123 uptake by flow cytometry as an indicator for cell viability. In addition, we measured intracellular ATP levels. No changes in cell viability or in intracellular ATP concentrations were observed during the course of the trans-stimulation

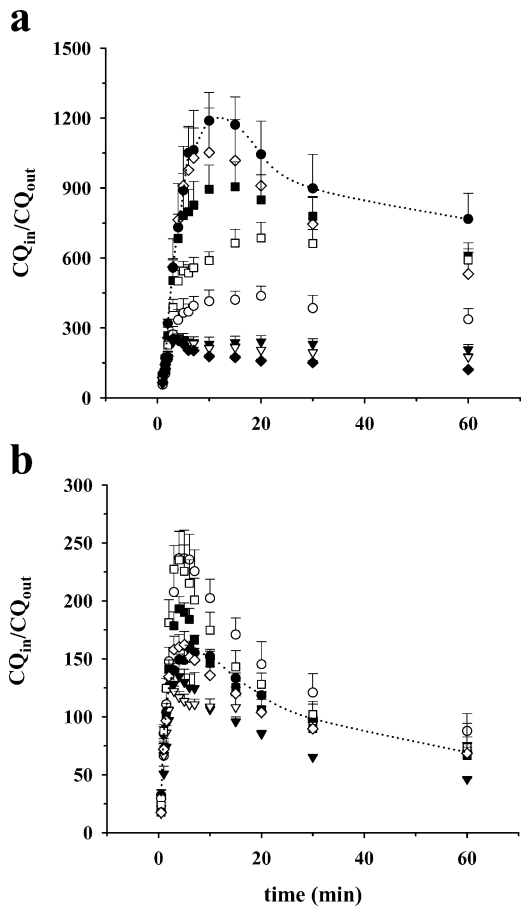

FIGURE 2: Chloroquine accumulation under trans-stimulation conditions. (a) CQS strain HB3. (b) CQR strain Dd2. Cells were pre-equilibrated in medium containing the following chloroquine concentrations: 0 (●); 0.1 μM (◇); 0.25 μM (■); 0.5 μM (□); 1.0 μM (○); 2.5 μM (▼); 5.0 μM (▽); 10.0 μM (◆). After preloading, cells were placed in medium containing radiolabeled chloroquine, and the time course of label uptake was monitored. Chloroquine uptake is expressed in terms of the ratio of the intracellular versus the extracellular [^{3}H]-chloroquine concentration, CQ_{in}/CQ_{out}. The data points for the controls, cells that were not pre-equilibrated with unlabeled chloroquine, are connected by dotted lines. The means ± SE of three or more independent determinations are shown.

experiments or between control and chloroquine-preloaded cells (data not shown). Thus, the differences seen between HB3 and Dd2 under these trans-stimulation conditions cannot be explained by differences in cell viability or a correlation between the IC_{50} value and probing chloroquine concentration. Instead, they seem to be a direct consequence of the parasites' different handling of the drug.

To study the trans-stimulation effect further, we analyzed the data obtained at times leading up to the uptake maximum in Figure 2, a and b. We fitted the uptake curves to simple rising exponentials for the first 7 min for the CQS data and the first 5 min for the CQR data. Essentially similar data were found if we fitted the data for the CQS strain for the first 5 min only, but we chose the longer time for further analysis because the CQS cells take longer to reach the maximum in chloroquine uptake. In Figure 3, a and b, are plots of the plateau values found for these data (essentially the maxima in the accumulation curves for each chloroquine concentration) against the equilibrium extracellular chloroquine concentration of each preloading condition. The equilibrium chloroquine concentration in the preloading medium was used instead of the initial preloading chloroquine concentration to take into account that the parasites take up substantial amounts of the drug from the medium during the preloading phase. The extracellular chloroquine concentration at equilibrium was determined for each preloading condition in independent experiments by using an appropriate concentration of [^{3}H]-chloroquine.

This analysis underscores the difference between the results for the CQS and for the CQR strain investigated. In HB3, the accumulated chloroquine falls continuously as the concentration of pre-equilibrated chloroquine rises. In Dd2, by contrast, the accumulation first rises and then falls with rising levels of pre-equilibrated chloroquine. The smooth lines through the points are obtained by curve fitting. The models used in these curve fits and the derived equations based on them are given in the Experimental Procedures and are described in the Discussion.

Trans-Stimulation Effect Is Energy Dependent. To investigate whether the energy-dependent chloroquine efflux and the trans-stimulation effect (both phenomena being observed for the CQR strain Dd2) are linked, we performed a series of trans-stimulation experiments with cells held in glucose-rich and glucose-free medium. Cells held in the glucose-free medium were glucose-starved before preloading with chloroquine and remained starved during the subsequent uptake of label. Accumulation of [^{3}H]-chloroquine under trans-stimulation conditions was determined at the 4 min time point only and analyzed as a function of the equilibrium chloroquine concentration in the corresponding preloading medium, as described above (Figure 4). In the glucose-rich medium, a trans-stimulation effect is observed with Dd2 but not with HB3, consistent with the data shown in Figures 2 and 3. The trans-stimulation effect, however, is lost in Dd2 when the experiment was conducted with glucose-starved cells. Now, the uptake of labeled chloroquine drops with increasing chloroquine in the preloading solutions and is parallel in both the CQS strain HB3 and the CQR strain Dd2 (Figure 4, c and d). The amount of labeled chloroquine taken up by the glucose-starved cells in the absence of preloaded chloroquine is consistent with the data in Figure 1 before addition of glucose. Apparently, to see the rise and fall in chloroquine accumulation with increasing preloaded chloroquine in the CQR strain Dd2, an energy input is needed.

Energy-Dependent Efflux and Trans Stimulation Are Associated with Chloroquine Resistance. To test whether the phenomena described above were, or were not, confined to the two strains investigated up to now, we performed a similar set of experiments with the CQS clone S106 (IC_{50} = 36.0 ± 4.0 nM) and the CQR clone FCB (IC_{50} = 131.0 ± 11.0 nM). According to recent studies, this is a matched pair of strains with a high degree of genetic similarity (*58*, *63*). A subtle, but important genetic difference between the two lies in their *pfcrt* genes, which differ by only a single nucleotide, rendering S106 chloroquine sensitive (*58*). Whereas FCB harbors the *pfcrt* allele causatively linked with the chloroquine-resistance phenotype (*38*, *64*, *65*), S106 appears to have resulted from a reversion event in which the amino acid Thr found in the CQR PfCRT protein at position 76 was changed back to the wild-type Lys (*38*, *58*).

Under conditions of glucose starvation, both S106 and FCB take up labeled chloroquine with comparable rates (Table 1). After the addition of glucose, however, chloroquine flux in the CQS and CQR strains is once again

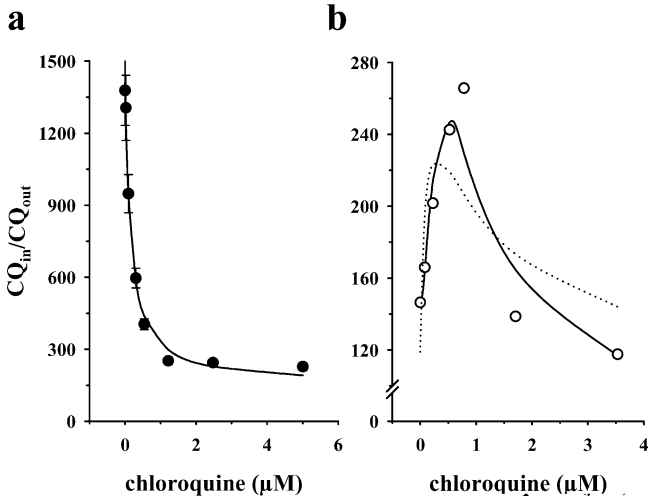

FIGURE 3: Effect of preloading with unlabeled chloroquine on [^{3}H]-chloroquine uptake in the CQS strain HB3 and the CQR strain Dd2. The maxima in the accumulation curves for each pre-equilibrated chloroquine concentration were calculated from Figure 2 and analyzed as a function of the equilibrium chloroquine concentration during each preloading condition. Chloroquine accumulation is given as the ratio of the intracellular versus the extracellular [^{3}H]-chloroquine concentration, CQ_{in}/CQ_{out}. (a) HB3 (●). Data were fitted using eq 10, assuming a simple diffusion and binding model. (b) Dd2 (○). The data were fitted using eq 11, assuming that the resistant strain has an additional energy-dependent efflux pump that moves chloroquine out of the compartment where it accumulates. The solid line represents a model where the pump expels two chloroquine molecules per pump cycle, and the dotted line represents a model where the pump expels one chloroquine molecule per cycle. The means ± SE of three or more independent determinations are shown. In some cases, the error bars are smaller than the size of the circles and are, for this reason, not visible in the graph.

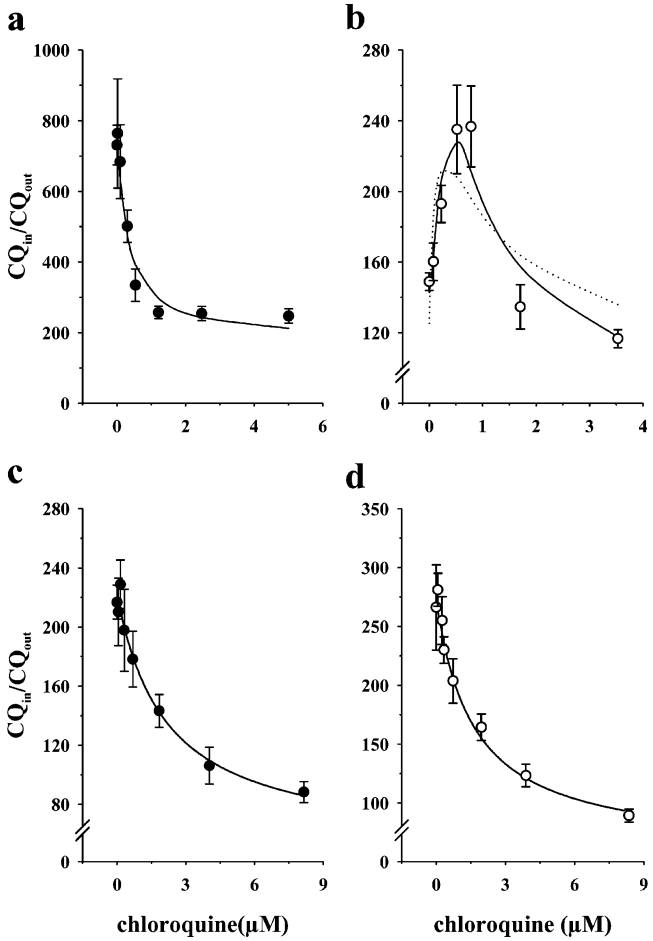

FIGURE 4: Effect of an energy input on trans-stimulated chloroquine uptake in the *P. falciparum* strains HB3 (a and c) and Dd2 (b and d). [^{3}H]-Chloroquine accumulation after 4 min of incubation with the label (given as the ratio of the intracellular versus the extracellular [^{3}H]-chloroquine concentration, CQ_{in}/CQ_{out}, at that time point) was analyzed as a function of the pre-equilibrium chloroquine concentration. Uptake studies were performed in glucose-rich medium (a and b) and glucose-free medium (c and d). The data represent the means ± SE of four or more independent determinations. The data were analyzed by curve fitting, using eq 10 for the data presented in a, c, and d and using eq 11 for the data presented in b. The solid line in b assumes a chloroquine pump with cooperative activity (Hill factor = 2), and the dotted line assumes a pump that transports only one chloroquine per cycle. The kinetic parameters obtained by curve fitting are compiled in Table 3.

fundamentally different between strains, here S106 and FCB. While S106 accumulates chloroquine further, FCB reduces its intracellular drug level when energized (Figure 5, a and b). The different handling of chloroquine is also revealed under trans-stimulation conditions. In the CQS strain S106, the drop in accumulation of the [^{3}H]-chloroquine is continuous with increasing preloaded chloroquine, whereas for the CQR strain FCB, the accumulation of labeled chloroquine first rises and then falls with increasing drug in the preloading solutions (Figure 5, c and d). These data are consistent with the concept that CQR strains have acquired an energy-dependent chloroquine efflux mechanism.

The Drug Efflux Model Is Consistent with Existing Kinetic Data on Chloroquine Accumulation. The observation that the apparent binding affinity of chloroquine to heme is reduced in CQR strains as compared to that in CQS strains (*20*, *60*) has been interpreted as evidence for a model in which chloroquine resistance is brought about by a heme-binding protein, which controls access of chloroquine to its target (*20*, *51*, *52*). However, would not an outwardly directed chloroquine pump have the same effect on chloroquine accumulation kinetics? To test this hypothesis, we measured chloroquine accumulation rates as a function of the external chloroquine concentration in the CQS strains HB3 and S106 and in the CQR strains Dd2 and FCB (Figure 6). The data obtained are comparable to those described by Bray et al. (*20*). We then fitted the data using our kinetic model, that is, uptake of chloroquine by diffusion and binding to identical intracellular targets and under identical pH gradients in CQS and CQR strains, whereas for the CQR strains it is additionally assumed that they have an energy-dependent chloroquine efflux carrier. As seen in Figure 6, our model fits the data of both the CQS and the CQR strains investigated with high confidence. Thus, the efflux carrier model is fully consistent with existing data on chloroquine accumulation kinetics described in the literature.

DISCUSSION

The data presented in Figure 1 are compatible with most, if not all, models that attempt to account for chloroquine resistance. They simply demonstrate that some energy-dependent mechanism leads to the loss of chloroquine from resistant cells but leads to its accumulation in the sensitive cells. The trans-stimulation experiments depicted in Figure 2 are, however, more discriminatory. It is clear from Figure 2, and even more so from Figures 3−5, that preloading cells

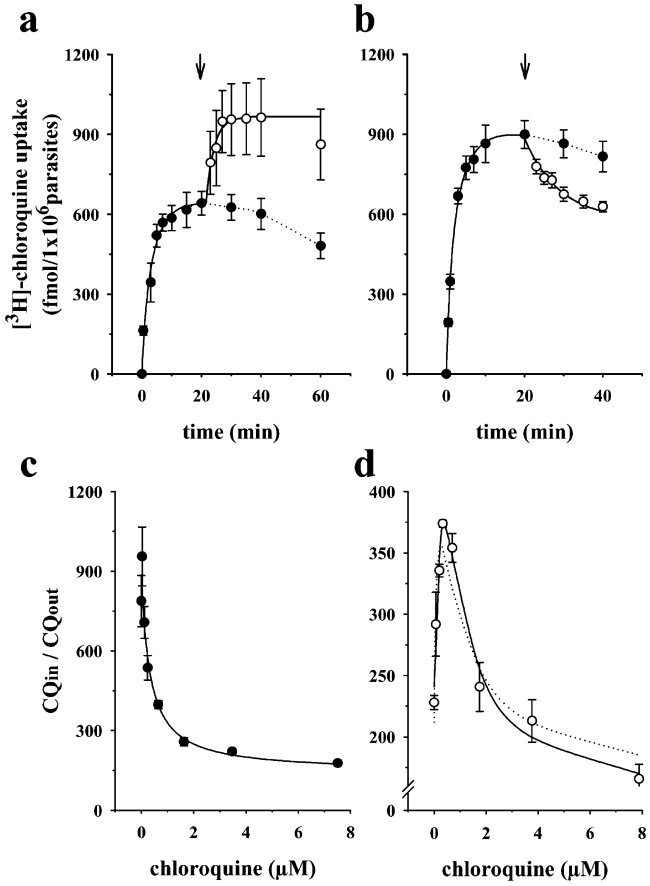

FIGURE 5: Energy-dependent chloroquine flux and trans-stimulated chloroquine uptake in the CQS strain S106 and the CQR strain FCB. Energy dependence of chloroquine flux was monitored in the CQS strain S106 (a) and the CQR strain FCB (b) in the presence (○) and absence of glucose (●). An arrow indicates the time point of glucose addition. Data points used for curve fitting are connected by a solid line. The kinetic parameters obtained by curve fitting are compiled in Table 1. (c and d) Trans-stimulated chloroquine uptake in S106 (c) and FCB (d). [^{3}H]-chloroquine accumulation after 4 min of incubation with the label (given as the ratio of the intracellular versus the extracellular [^{3}H]-chloroquine concentration, CQ_{in}/CQ_{out}, at that time point) was analyzed as a function of the pre-equilibrium chloroquine concentration. The data represent the means ± SE of four or more independent determinations. The data were analyzed by curve fitting, using eq 10 for the data presented in c and eq 11 for the data presented in d. The solid line in d assumes a chloroquine pump with cooperative activity (Hill factor = 2), and the dotted line assumes a pump that transports only one chloroquine per cycle. The kinetic parameters obtained by curve fitting are compiled in Table 3.

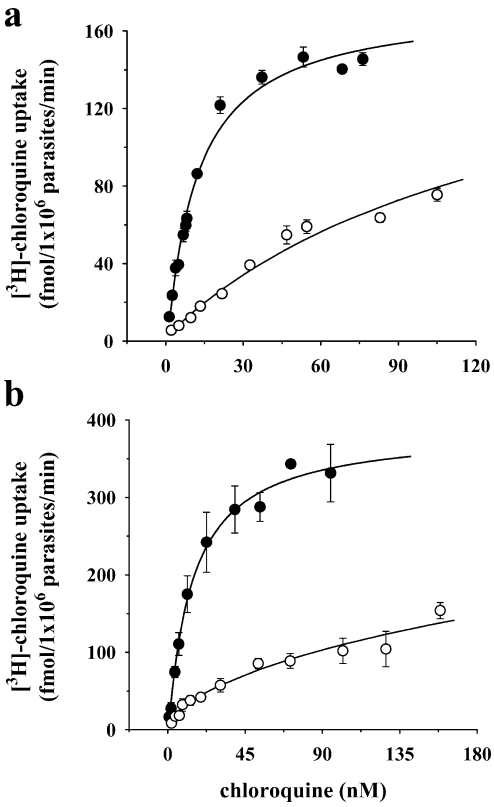

FIGURE 6: Kinetics of chloroquine uptake in different *P. falciparum* strains. Initial rates of chloroquine uptake (in fmol chloroquine/1 × 10^6 parasites/min) were analyzed as a function of different extracellular chloroquine concentrations. (a) HB3 (●) and Dd2 (○). (b) S106 (●) and FCB (○). The data represent the means ± SE of three or more independent determinations. The data for the CQS strains HB3 and S106 were curve fitted using eq 1, assuming a simple diffusion and binding model. The data for the CQR strains Dd2 and FCB were curve fitted by using eq 4, assuming that a pump expels chloroquine from the compartment where it accumulates. The kinetic parameters obtained by curve fitting are compiled in Table 2.

with chloroquine has a qualitatively different effect in CQS than in CQR strains, irrespective of the probing [^{3}H]-chloroquine concentration. In CQS strains, each additional increment of chloroquine within the cells leads to a drop in the accumulation of labeled chloroquine. This is compatible with the internal chloroquine competing with incoming label for binding to some intraparasitic binding site or binding process. This could be binding to heme present in the parasite vacuole, as cogently argued for by Bray et al. (*20*, *51*). With a turnover rate of 0.06 fmol/h of hemoglobin (*66*), each parasite produces sufficient heme to account for the chloroquine accumulation observed in CQS strains (*67*). Alternatively, the chloroquine could be held within the vacuole as the diprotonated form, its accumulation being dependent on the vacuolar pH (*41*). In the latter case, excess chloroquine within the vacuole might deplete the pH gradient and lead to a lowered extent of accumulation.

In the case of the CQR cells, however, low levels of preloaded chloroquine lead to an *increase* in the extent of accumulation of the drug. Only at the higher levels of preloaded chloroquine does the extent of accumulation begin to fall below the maximal level, eventually reaching a level lower than that of the control (in the absence of preloaded chloroquine). Can this be accounted for by a model in which chloroquine resistance is brought about by a model in which a heme-binding protein diminishes the binding affinity of chloroquine to heme? It is perhaps possible that a version of the binding diminution model might be able to fit these data, but we ourselves have not been able to come up with such a model. No change in the affinity of chloroquine for some intracellular binding component nor the presence of additional chloroquine-binding sites would account for the data in Figures 2−5. Nor is it likely that a reduced accumulation in the vacuole, due to a pH difference between CQS and CQR strains, is the explanation since it is hard to see why, in CQR strains, low levels of preloaded chloroquine should give rise to an increased pH gradient (giving rise to increased accumulation) while higher levels of the same drug should have the opposite effect. Again, if the change in vacuolar pH leads to a reduction in the amount of heme

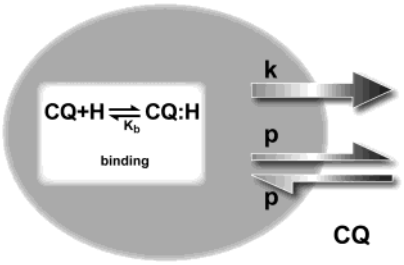

FIGURE 7: Proposed model of chloroquine resistance in *P. falciparum*. Chloroquine, CQ, enters and leaves the compartment where it accumulates by a simple bidirectional leak, having the rate constant *p* for drug movement in both directions. In addition, intracellular chloroquine is bound within this compartment to some binding site, *H*, forming a stable complex, termed CQ:H, with a binding affinity given by the dissociation constant (Michaelis constant), K_b. In chloroquine-resistant strains, chloroquine is pumped out of this compartment by an energy-dependent pump having the rate constant *k*.

available as targets for chloroquine binding (*45*−*47*), a convoluted explanation will be needed to explain how a steadily rising level of internal chloroquine first depresses heme aggregation and crystallization and then improves it.

The data of Figures 2−5 (and also Figure 6) are direct predictions, however, of the very simple model that shows that an energy-dependent, outwardly directed chloroquine efflux mechanism is responsible for chloroquine resistance in the CQR strains. At low levels, the pre-equilibrated unlabeled chloroquine will compete, on the carrier, with the labeled chloroquine that has entered by simple diffusion, blocking *efflux* of labeled chloroquine and hence increasing the net entry of the label. This is the well-known trans-acceleration phenomenon, which has been unequivocally shown to be characteristic of saturable, carrier-mediated transport systems (*62*). It will not be found for a system in which the substrate moves across the cell membrane by diffusion (whether through the lipid phase of the membrane or through pores) and is merely held within the compartment in which it accumulates by binding to some internal component or is redistributed there by a standing pH gradient (*62*). Trans acceleration is, however, a natural consequence of the intervention of some carrier-mediated process in the energy-dependent transport of chloroquine out of the compartment into which it accumulates. At the higher levels of preloaded chloroquine, the postulated carrier is already fully inhibited, and the unlabeled chloroquine, by competing for binding to the chloroquine-binding sites, now reduces the extent of accumulation of labeled chloroquine, exactly as it does for the CQS strains.

On the basis of our data, we propose that the acquisition of an energy-dependent carrier-mediated efflux system is a minimal and necessary event in the generation of the chloroquine-resistant phenotype in *P. falciparum*. This carrier would extrude chloroquine from the compartment where it accumulates (Figure 7). Chloroquine would enter this compartment by a simple bidirectional leak, through the lipid phase of the membrane or through pores, in a manner similar to that in CQS strains (Figure 7). The chloroquine efflux carrier could be a primary active transporter, such as a pump, or a secondary active transporter that co- or counter-transports chloroquine with or against a substrate.

A kinetic model designed for a situation where intracellular accumulation of a substance is counteracted by an efflux system (*68*) was applied to chloroquine accumulation in *P. falciparum* to verify the interpretation of our data. As seen from the lines drawn in Figures 3−6, fairly good fits to the appropriate equations (eqs 10 and 11 and 1 and 4) were found, especially when a cooperativity of 2 was assumed for the action of the efflux carrier on chloroquine (the solid lines in Figures 3b and 4b). A stoichiometry of two chloroquine molecules per carrier cycle is preferred statistically at the 5% level of significance for the data presented in Figures 3b and 4b. The efflux model thus has no trouble in predicting the results of the trans-stimulation experiments and the chloroquine-uptake kinetics for both CQS and CQR cells. Note that for these curve fits we have taken the simple standpoint that sensitive and resistant strains differ only in the fact of the absence or presence of the chloroquine efflux carrier. Because we can fit all our data on this simple assumption, we have not attempted fits in which the chloroquine-binding sites, the prevailing pH gradients, or the relative volume of the food vacuole differs between sensitive and resistant strains. They may indeed differ between different *P. falciparum* strains or between CQS and CQR strains, but this will not affect the overall outcome or the interpretation of the trans-stimulation experiments (see above). It should further be noted that our model, in the form of eqs 1 and 4, perfectly fits published kinetic data for steady-state and initial chloroquine accumulations in CQS and CQR strains, similar to those shown in Figure 6. Thus, our data are fully consistent with the concept that CQR strains control access of chloroquine to heme, as stressed by Bray et al. (*20*). Yet, the underlying mechanism is a drug efflux pump, which serves to reduce the intracellular chloroquine concentration, and not a heme-binding protein that diminishes the intrinsic drug-binding constant to heme.

Table 2: Kinetic Parameters for Initial Chloroquine Uptake in Different *P. falciparum* Strains[a]

strain	status	K_b (binding) nM	r_o (pump/leak)	K_p (pumping) nM
HB3	CQS	14.1 ± 1.1 (7)		
S106	CQS	15.7 ± 2.8 (3)		
Dd2	CQR	84.0 ± 12.0 (5)[b]	9.9 ± 0.5 (5)	0.27 ± 0.19 (5)
FCB	CQR	60.0 ± 20.0 (6)[b]	28.0 ± 10.0 (6)	4.0 ± 3.2 (6)

[a] The values represent the means ± SE of *n* independent determinations and are derived from curve fitting of the data shown in Figure 6. K_b, dissociation constant between chloroquine and its intracellular binding site (Michaelis constant); K_p, apparent binding constant of chloroquine to the efflux carrier (Michaelis constant); r_o, pump-to-leak ratio. [b] Assuming no pumping.

The curve fits yielded kinetic parameters for the dissociation constant between chloroquine and its intracellular binding site (Michaelis constant), K_b; the apparent binding constant of chloroquine to the postulated efflux carrier (Michaelis constant), K_p; and the pump-to-leak ratio, r_o (Tables 2 and 3). The K_b values obtained, by fitting the chloroquine uptake kinetics in Figure 6 using eq 4, are in the nM range, are consistent with previous reports (*20*, *60*), and are very similar for both the CQS strains HB3 and S106 (14.1 ± 1.1 and 15.7 ± 2.8, all values in nM). For the CQR strains, the following values for r_o and K_p were obtained: $r_o = 9.9 \pm 0.5$ and $K_p = 0.27 \pm 0.19$ for Dd2; and $r_o = 28.0 \pm 10.0$ and $K_p = 4.0 \pm 3.2$ for FCB.

The values for the constants K_b and K_p found by curve fits in the trans-stimulation experiments in Figures 3−5

Table 3: Kinetic Parameters for Chloroquine Uptake under Trans-Stimulation Conditions in Different *P. falciparum* Strains[a]

strain	status	K_b (binding) nM	r_o (pump/leak)	K_p (pumping) nM
HB3	CQS	300 ± 108 (3)[b]		
S106	CQS	330 ± 140 (4)[b]		
Dd2	CQR		16.8 ± 4.4 (4)	2.0 ± 1.3 (4)
FCB	CQR		14.8 ± 2.0 (5)	1.6 ± 0.6 (5)

[a] The values represent the means ± SE of *n* independent determinations and are derived from curve fitting of the data shown in Figures 4 and 5. K_b, dissociation constant between chloroquine and its intracellular binding site (Michaelis constant); K_p, apparent binding constant of chloroquine to the efflux carrier (Michaelis constant); r_o, pump-to-leak ratio. [b] These estimates are based on the equilibrium chloroquine concentrations during preloading, which are necessarily higher than those actually seen by the cells by 4 min of labeled chloroquine uptake.

(Table 3) should be considered as being of only qualitative significance. They are determined in terms of the concentration of the equilibrium chloroquine in the preloading medium, as denoted on the abscissas of Figures 3−5. After loading, however, some 50% of the drug is lost in the washing procedure before the cells are exposed to labeled chloroquine. Then during the uptake of label, further chloroquine is lost, up to 50% in some experiments in the CQR cells and up to 40% in the CQS cells. Thus, the derived K_b and K_p values could be somewhat overestimated by this preloading procedure. These considerations, that chloroquine preloading levels are overestimated, should not affect the determinations of the maximum capacity of the chloroquine entry process nor the estimate of the pump-to-leak ratio. The former is measured at saturating chloroquine levels; therefore, it is independent of any errors in measuring absolute chloroquine levels. The latter essentially derives from the ratios of drug uptakes in the two strains in the absence of preloading and is again independent of the values of the ambient drug concentrations. The values found for all the parameters are, of course, strictly model-dependent. Interestingly, the values of the pump-to-leak ratio, r_o, found by the initial uptake procedure of Figure 6 (Table 2), are not very different from the estimates derived from the trans-stimulation experiments of Figures 3−5 (Table 3). For Dd2, the r_o values are 9.9 ± 0.5 (initial uptake procedure) and 16.8 ± 4.4 (trans stimulation); for FCB the r_o values are 28.0 ± 10.0 (initial uptake procedure) and 14.8 ± 2.0 (trans stimulation).

Curve fitting of the time course of chloroquine uptake in Figures 1 and 5 gives the rate constants for the entry processes. Uptake is rapid, with half-lives of some 1−2 min for parasites in the absence of glucose or for the sensitive strains after glucose addition (Table 1). Chloroquine efflux in the resistant strains investigated is, however, a slower process with a half-life of some 6 min. That this is very close to the 6 min found for the half-life of the restoration of ATP levels after glucose addition might suggest that it is the level of intracellular ATP that is rate limiting for the efflux process. If the postulated chloroquine efflux carrier is a primary active transporter (*62*), then the postulated pump has a rather low affinity for ATP, in that a small rise in the intracellular ATP level is not sufficient to activate it fully. If the chloroquine efflux carrier is a secondary active transporter (*62*), then the time course being measured should be related to the need for establishing the transmembrane gradient of the substrate that drives chloroquine transport. The rapid rise in accumulated chloroquine after glucose addition in the CQS strains seems to be activated at lower levels of intracellular ATP. This would be consistent with the increased chloroquine uptake after glucose addition in the CQS strains being dependent on an energy input for hemoglobin degradation and, hence, the production of free heme as target for chloroquine binding or, alternatively, being dependent on proton accumulation in the vacuolar compartment into which it accumulates (*41*), with proton pumping being performed by a pump of high affinity for ATP. In the CQR strains, the activation of the chloroquine efflux carrier by glucose addition counteracts the effect of the increased driving force for chloroquine accumulation.

We have tried to be careful in this paper not to specify the physical location in the cell into which chloroquine is accumulated and from which it is, we postulate, pumped. The consensus of evidence indicates that it is bound to heme within the vacuole (*2*, *47*). None of our evidence has bearing upon this point, nor were any of our experiments designed to test this hypothesis. The same can be said for the location of the drug efflux carrier that we postulate is acting to decrease the chloroquine level in the compartment in which chloroquine accumulates. If chloroquine does accumulate within the acidic food vacuole in CQS cells, then a reasonable location for the chloroquine efflux carrier would be at the vacuole/parasite cytoplasm membrane. We do not think, however, that the interpretation of our data would be any different if the carrier were situated at the membrane between the parasite and the red cell. We do not have any information on this important point.

Our evidence for the existence of an energy-dependent efflux carrier for chloroquine is purely kinetic in nature and does not reveal its molecular identity. One might begin to speculate as to which of the proteins linked with chloroquine resistance in *P. falciparum* mediates the drug efflux phenotype. One candidate is Pgh1, the *P. falciparum* homologue of the human P-glycoprotein mediating multidrug resistance in cancer cells (*24*). Encoded by *Pfmdr1*, Pgh1 is located on the food vacuolar membrane and, to a lesser extent, on the parasite plasma membrane (*69*). Amplification of *Pfmdr1* is not associated with chloroquine resistance in *P. falciparum* (*70*), and epidemiological studies have suggested only a vague correlation of chloroquine resistance with mutations within this gene (*23*, *31*−*33*). However, allelic exchange experiments, where the *mdr1* allele of a CQR strain was replaced by that of a CQS strain and vice versa, showed that the reported mutations within *Pfmdr1* affect the degree of chloroquine resistance, albeit are insufficient to bring about the chloroquine resistance phenotype per se (*71*).

A second candidate protein is the *P. falciparum* chloroquine resistance transporter PfCRT (*38*). Like Pgh1, PfCRT is located on the food vacuolar membrane where it may play a role as a chloride channel or transporter (*72*, *73*). Mutations within *Pfcrt* are causatively linked with chloroquine resistance, as has been shown in a genetic cross done with HB3 and Dd2 (*38*), in reverse genetic studies (*64*), in drug selection studies (*58*), and in epidemiological surveys (*65*). Our finding that the two matched strains, FCB and S106, which differ only by a single amino acid exchange (Thr 76 Lys) in PfCRT in an otherwise highly similar genetic background (*58*), handle chloroquine differently further

points toward PfCRT as a crucial factor in constituting the efflux pump associated with chloroquine resistance in *P. falciparum*. However, it would be premature to conclude that PfCRT itself is the chloroquine efflux carrier. Alternatively, PfCRT may function as an activator of the drug carrier.

ACKNOWLEDGMENT

We thank Dr. Hagai Ginsburg for advice and critical discussions and Elisabeth Wilken and Kathrin Steigleder for technical assistance.

REFERENCES

1. World Health Organization. *Technical Report Series 892*, (2000) i−v, 1−74.
2. Foley, M., and Tilley, L. (1998) *Pharmacol. Ther. 79*, 55−87.
3. Surolia, N., and Padmanaban, G. (1991) *Proc. Natl. Acad. Sci. U.S.A. 88*, 4786−4790.
4. Surolia, I. (2000) *Parasitol. Today 16*, 133.
5. Sugioka, Y., Suzuki, M., Sugioka, K., and Nakano, M. (1987) *FEBS Lett. 223*, 251−254.
6. Ginsburg, H., and Demel, R. A. (1983) *Biochim. Biophys. Acta 732*, 316−319.
7. Loria, P., Miller, S., Foley, M., and Tilley, L. (1999) *Biochem. J. 339* (*Pt 2*), 363−370.
8. Zhang, J., Krugliak, M., and Ginsburg, H. (1999) *Mol. Biochem. Parasitol. 99*, 129−141.
9. Ginsburg, H., Famin, O., Zhang, J., and Krugliak, M. (1998) *Biochem. Pharmacol. 56*, 1305−1313.
10. Pagola, S., Stephens, P. W., Bohle, D. S., Kosar, A. D., and Madsen, S. K. (2000) *Nature 404*, 307−310.
11. Pandey, A. V., Bisht, H., Babbarwal, V. K., Srivastava, J., Pandey, K. C., and Chauhan, V. S. (2001) *Biochem. J. 355*, 333−338.
12. Moreau, S., Perly, B., Chachaty, C., and Deleuze, C. (1985) *Biochim. Biophys. Acta 840*, 107−116.
13. Zhang, Y., and Hempelmann, E. (1987) *Biochem. Pharmacol. 36*, 1267−1273.
14. Chou, A. C., and Fitch, C. D. (1980) *J. Clin. Invest. 66*, 856−858.
15. Fitch, C. D., Chevli, R., Banyal, H. S., Phillips, G., Pfaller, M. A., and Krogstad, D. J. (1982) *Antimicrob. Agents Chemother. 21*, 819−822.
16. Fitch, C. D., Chevli, R., Kanjananggulpan, P., Dutta, P., Chevli, K., and Chou, A. C. (1983) *Blood 62*, 1165−1168.
17. Orjih, A. U., Banyal, H. S., Chevli, R., and Fitch, C. D. (1981) *Science 214*, 667−669.
18. Lew, V. L., Tiffert, T., and Ginsburg, H. (2003) *Blood 101*, 4189−4194.
19. Slater, A. F., and Cerami, A. (1992) *Nature 355*, 167−169.
20. Bray, P. G., Mungthin, M., Ridley, R. G., and Ward, S. A. (1998) *Mol. Pharmacol. 54*, 170−179.
21. Fitch, C. D. (1970) *Science 169*, 289−290.
22. Fitch, C. D. (1973) *Antimicrob. Agents Chemother. 3*, 545−548.
23. Foote, S. J., Kyle, D. E., Martin, R. K., Oduola, A. M., Forsyth, K., Kemp, D. J., and Cowman, A. F. (1990) *Nature 345*, 255−258.
24. Foote, S. J., Thompson, J. K., Cowman, A. F., and Kemp, D. J. (1989) *Cell 57*, 921−930.
25. Krogstad, D. J., Gluzman, I. Y., Kyle, D. E., Oduola, A. M., Martin, S. K., Milhous, W. K., and Schlesinger, P. H. (1987) *Science 238*, 1283−1285.
26. Martin, S. K., Oduola, A. M., and Milhous, W. K. (1987) *Science 235*, 899−901.
27. Wilson, C. M., Serrano, A. E., Wasley, A., Bogenschutz, M. P., Shankar, A. H., and Wirth, D. F. (1989) *Science 244*, 1184−1186.
28. Bray, P. G., Howells, R. E., Ritchie, G. Y., and Ward, S. A. (1992) *Biochem. Pharmacol. 44*, 1317−1324.
29. Bray, P. G., Hawley, S. R., and Ward, S. A. (1996) *Mol. Pharmacol. 50*, 1551−1558.
30. von Seidlein, L., Duraisingh, M. T., Drakeley, C. J., Bailey, R., Greenwood, B. M., and Pinder, M. (1997) *Trans. R. Soc. Trop. Med. Hyg. 91*, 450−453.
31. Mungthin, M., Bray, P. G., and Ward, S. A. (1999) *Am. J. Trop. Med. Hyg. 60*, 469−474.
32. McCutcheon, K. R., Freese, J. A., Frean, J. A., Sharp, B. L., and Markus, M. B. (1999) *Trans. R. Soc. Trop. Med. Hyg. 93*, 300−302.
33. Bhattacharya, P. R., and Pillai, C. R. (1999) *Ann. Trop. Med. Parasitol. 93*, 679−684.
34. Bhattacharya, P. R., Biswas, S., and Kabilan, L. (1997) *Trans. R. Soc. Trop. Med. Hyg. 91*, 454−455.
35. Basco, L. K., and Ringwald, P. (1998) *Am. J. Trop. Med. Hyg. 59*, 577−581.
36. Basco, L. K., de Pecoulas, P. E., Le Bras, J., and Wilson, C. M. (1996) *Exp. Parasitol. 82*, 97−103.
37. Wellems, T. E., Panton, L. J., Gluzman, I. Y., do Rosario, V. E., Gwadz, R. W., Walker-Jonah, A., and Krogstad, D. J. (1990) *Nature 345*, 253−255.
38. Fidock, D. A., Nomura, T., Talley, A. K., Cooper, R. A., Dzekunov, S. M., Ferdig, M. T., Ursos, L. M., Sidhu, A. B., Naude, B., Deitsch, K. W., Su, X. Z., Wootton, J. C., Roepe, P. D., and Wellems, T. E. (2000) *Mol. Cells 6*, 861−871.
39. Yayon, A., Cabantchik, Z. I., and Ginsburg, H. (1984) *EMBO J. 3*, 2695−2700.
40. Yayon, A., Cabantchik, Z. I., and Ginsburg, H. (1985) *Proc. Natl. Acad. Sci. U.S.A. 82*, 2784−2788.
41. Ginsburg, H., and Stein, W. D. (1991) *Biochem. Pharmacol. 41*, 1463−1470.
42. Spiller, D. G., Bray, P. G., Hughes, R. H., Ward, S. A., and White, M. R. (2002) *Trends Parasitol. 18*, 441−444.
43. Krogstad, D. J., Schlesinger, P. H., and Gluzman, I. Y. (1985) *J. Cell Biol. 101*, 2302−2309.
44. Krogstad, D. J., Gluzman, I. Y., Herwaldt, B. L., Schlesinger, P. H., and Wellems, T. E. (1992) *Biochem. Pharmacol. 43*, 57−62.
45. Dzekunov, S. M., Ursos, L. M., and Roepe, P. D. (2000) *Mol. Biochem. Parasitol. 110*, 107−124.
46. Ursos, L. M., DuBay, K. F., and Roepe, P. D. (2001) *Mol. Biochem. Parasitol. 112*, 11−17.
47. Ursos, L. M., and Roepe, P. D. (2002) *Med. Res. Rev. 22*, 465−491.
48. Bray, P. G., Saliba, K. J., Davies, J. D., Spiller, D. G., White, M. R., Kirk, K., and Ward, S. A. (2002) *Mol. Biochem. Parasitol. 119*, 301−304; discussion 307−309, 311−313.
49. Wissing, F., Sanchez, C. P., Rohrbach, P., Ricken, S., and Lanzer, M. (2002) *J. Biol. Chem. 277*, 37747−37755.
50. Wellems, T. E., Wootton, J. C., Fujioka, H., Su, X., Cooper, R., Baruch, D., and Fidock, D. A. (1998) *Cell 94*, 285−286.
51. Bray, P. G., Janneh, O., and Ward, S. A. (1999) in *Transport and Trafficking in the Malaria-Infected Erythrocyte* (Bock, G. R., and Cardew, G., Eds.) Novartis Foundation Symposium 226, Wiley & Sons, Chichester, NY, pp 252−260.
52. Raynes, K. J., Bray, P. G., and Ward, S. A. (1999) *Drug Resist. Updates 2*, 97−103.
53. Sullivan, D. J., Jr., Gluzman, I. Y., and Goldberg, D. E. (1996) *Science 271*, 219−222.
54. Staalsoe, T., Giha, H. A., Dodoo, D., Theander, T. G., and Hviid, L. (1999) *Cytometry 35*, 329−336.
55. Trager, W., and Jensen, J. B. (1976) *Science 193*, 673−675.
56. Lambros, C., and Vanderberg, J. P. (1979) *J. Parasitol. 65*, 418−420.
57. Su, X. Z., Carucci, D. J., and Wellems, T. E. (1998) *Exp. Parasitol. 89*, 262−265.
58. Cooper, R. A., Ferdig, M. T., Su, X. Z., Ursos, L. M., Mu, J., Nomura, T., Fujioka, H., Fidock, D. A., Roepe, P. D., and Wellems, T. E. (2002) *Mol. Pharmacol. 61*, 35−42.
59. Saliba, K. J., Horner, H. A., and Kirk, K. (1998) *J. Biol. Chem. 273*, 10190−10195.
60. Sanchez, C. P., Wunsch, S., and Lanzer, M. (1997) *J. Biol. Chem. 272*, 2652−2658.
61. Diribe, C. O., and Warhurst, D. C. (1985) *Biochem. Pharmacol. 34*, 3019−3027.
62. Stein, W. D. (1986) *Transport and Diffusion across Cell Membranes*, Academic Press, NY.
63. Su, X., Kirkman, L. A., Fujioka, H., and Wellems, T. E. (1997) *Cell 91*, 593−603.
64. Sidhu, A. B., Verdier-Pinard, D., and Fidock, D. A. (2002) *Science 298*, 210−213.
65. Djimde, A., Doumbo, O. K., Cortese, J. F., Kayentao, K., Doumbo, S., Diourte, Y., Dicko, A., Su, X. Z., Nomura, T., Fidock, D. A., Wellems, T. E., Plowe, C. V., and Coulibaly, D. (2001) *N. Engl. J. Med. 344*, 257−263.

66. Goldberg, D. E., Slater, A. F., Beavis, R., Chait, B., Cerami, A., and Henderson, G. B. (1991) *J. Exp. Med. 173*, 961−969.
67. Bray, P. G., Janneh, O., Raynes, K. J., Mungthin, M., Ginsburg, H., and Ward, S. A. (1999) *J. Cell Biol. 145*, 363−376.
68. Stein, W. D. (1997) *Physiol. Rev. 77*, 545−590.
69. Cowman, A. F., Karcz, S., Galatis, D., and Culvenor, J. G. (1991) *J. Cell Biol. 113*, 1033−1042.
70. Barnes, D. A., Foote, S. J., Galatis, D., Kemp, D. J., and Cowman, A. F. (1992) *EMBO J. 11*, 3067−3075.
71. Reed, M. B., Saliba, K. J., Caruana, S. R., Kirk, K., and Cowman, A. F. (2000) *Nature 403*, 906−909.
72. Zhang, H., Howard, E. M., and Roepe, P. D. (2002) *J. Biol. Chem. 277*, 49767−49775.
73. Warhurst, D. C., Craig, J. C., and Adagu, I. S. (2002) *Lancet 360*, 1527−1529.

BI034269H